ANALYSIS OF THE STATIC AND DYNAMIC AERO-STRUCTURAL RESPONSE OF AN ELASTIC SWEPT WING MODEL BY DIRECT AEROELASTIC SIMULATION

L. Reimer*, C. Braun**, J. Ballmann**

* Chair for Computational Analysis of Technical Systems (CATS), Steinbach-strasse 53B, 52074 Aachen, Germany, RWTH Aachen University

** Department of Mechanics (LFM), Templergraben 64, 52062 Aachen, Germany, RWTH Aachen University

Keywords: *Numerical Aeroelasticity*

Abstract

In this report the numerical method SOFIA for direct aeroelastic simulation is applied to a swept wing wind tunnel configuration in the subsonic flow regime. The computational results reveal a good aggreement of the deformations and clamping reactions predicted by SOFIA with the performed wind tunnel results. This is valid for the aeroelastic equilibrium configuration as well as for the dynamic response tests.

1 Introduction

Lightweight structures of airplane wings and concurrent rising transport capacities of modern aircrafts require powerful and safe tools, which reliably predict the interaction between aerodynamic, inertial and structural forces. Since dynamic instabilities can cause a rapid growth of vibration amplitudes of elastic, lift generating structures, it is essential to analyse the characteristics of the coupled fluid-structure system under non-stationary conditions. For these purposes the numerical method SOFIA (SOlid Fluid InterAction) for direct numerical aeroelastic simulation is being progressively developed within the framework of the Collaborative Research Center SFB 401 "Flow Modulation and Fluid-Structure Interaction at Airplane Wings" at RWTH Aachen University [1]. SOFIA is based on a coupled multi-field formulation, in which solvers based on distinct numerical discretisation for fluid and structure are coupled.

Newly developed codes for computational aeroelastic analysis need extensive sets of wind tunnel data from experiments with elastic 3D wing models for validation. Due to the limited number of elastic wing models for public aerostructural research (at least in Europe), one objective of SFB 401 is to create data sets for benchmarking. Within this framework a flexible swept wing model has been designed and manufactured at the Institute for Lightweight Structures (ILB) at RWTH Aachen University [2] and was tested in the German-Dutch Low-Speed Wind Tunnels (DNW-LST) in Emmeloord (NL). The performed wind tunnel tests comprehended static aeroelastic experiments with analysis of aeroelastic equilibrium configurations as well as dynamic response tests in the subsonic flow regime. In all performed tests the root forces and moments, the spanwise deformation, consisting mainly of torsional twist and bending, and the pressure distribution at spanwise cross-sections have been recorded and are available for comparison with numerical results.

It is demonstrated in this report that the aeroelastic method SOFIA is capable to predict accurately the static deformation state and the dynamic response behaviour of the examined swept

wing wind tunnel model in combination with the corresponding surrounding flow field. It is shown in the static case that the computed bending deformation and the root forces are in excellent agreement with the measured data, whereas the torsional twist deformation and the root moments have been predicted insignificantly less accurate by the computations. The simulation of the dynamic response of the wing reveals that damping and frequency of the bending deformation are in very good conformance with the measured time history, whereas again the twist deformation shows an overestimation of the experimentally determined vibration amplitude.

2 Physical Models and Numerical Methods

The aeroelastic method SOFIA solves the coupled problem consisting of the flow field, the displacement field of the structure and the deformation of the flow grid. Due to its coupled multi-field formulation each of the identifiable fields is represented within SOFIA by an independent program component, which is specialized regarding the particular demands of the respective application in aeroelasticity. The essential communication between flow solver, structural solver and flow grid deformation method is managed via an aeroelastic coupling module developed for this purpose. The program components of the overall aeroelastic program system and the underlying physical models and numerical methods are described below.

2.1 Fluid Dynamics

In SOFIA the compressible, unsteady fluid flow involving viscosity and heat conduction is described by the three-dimensional Favre- and Reynolds-averaged Navier-Stokes (RANS) equations which are derived from the Navier-Stokes equations by applying mass and time averaging processes. The governing equations are solved approximately using the flow solver FLOWer, which has been developed in the project MEGAFLOW by different German research organisations under the direction of the German Aerospace Center DLR [3].

In the FLOWer code a finite volume technique for block-structured grids is applied, where the control volumina are dependent on time due to the deformation of the computational mesh. By coupling FLOWer with a sophisticated grid deformation method the computational mesh is deformed such that the nodes on the outer boundary may be freely movable or remain fixed, in the sense of a flow simulation in a wind tunnel fixed co-ordinate system, while the nodes lying on the wing surface are always moved accordingly to the displacement field of the surface. Thereby a body fitting grid is assured at any time [4, 5]. The time integration in FLOWer is performed by dual-time stepping. Within each pseudo-time step an explicit multi-stage Runge-Kutta method is used which is accelerated by techniques of local pseudo-time stepping and implicit residual smoothing. The solution procedure is embedded into a multigrid algorithm. The FLOWer code provides various algebraic and one- or two-equation turbulence models.

2.2 Structural Dynamics

In SOFIA the supporting elastic wing structure is modeled by a Timoshenko-like multi-axial beam with six degrees of freedom for a material cross-section. Multi-axial means that the centerlines of mass, bending and torsion may differ. In contrast to the often used Euler/Bernoulli beam theory which couples bending with translation by kinematic constraint and thus causes shear rigidity and anomalous dispersion of deformation energy propagation, the Timoshenko approximation with its two more degrees of freedom concerning the shear deformation exhibits no effects of anomalous dispersion and thus describes unsteady deformation with finite propagation speeds, which is physically reasonable.

For determining the generalized displacements of the structure, a system of ordinary differential equations (ODEs) of second order in time is derived from Hamilton's principle and applying a finite element (FE) approach. FE discretization is done by using two-noded beam el-

ements based on the formulation of shape functions (third/second order polynomials for translational/rotational motion related to bending, first order for torsion) described in [4], which is unsusceptible to shear locking. The set of ODEs is integrated using the Bossak scheme [6], where the resulting linear system of equations is solved iteratively using advanced ILU-type preconditioned Krylov sub-space methods. The external forces are assumed to vary linearly during every time step.

2.3   Flow Grid Deformation Method

In every time step of an aeroelastic computation the computational mesh for the flow solver has to be updated according to the change of shape of the wing surface. Therefore an algorithm has been developed, in which the block boundaries and an additional number of grid lines, which depend on the grid topology, are modeled such that a fictitious framework of elastic beams is formed [4, 5]. These beams are considered rigidly fixed together in points of intersection and on the aerodynamic surface as well. Thus, angles are preserved where grid lines, which are modeled as ficitious beams, intersect or emerge from a wetted surface. The deformation of the fictitious beam framework, which is linked to displacements of the surface grid nodes, is calculated by an FE solver. The new positions of grid points in the interior of the domain which are not included in the fictitious beam framework are determined via transfinite algebraic interpolation.

2.4   Aeroelastic Coupling Module

When using an aeroelastic method, which is based on a coupled multi-field formulation, the natural interface between the elastic structure and the surrounding fluid is the aerodynamic surface. Along this surface information connecting forces and displacements have to be exchanged between the distinct field solvers.

For these purposes a widely independent coupling module has been developed and implemented, which executes the data transfer between fluid solver and structural solver. Its concept en-

ables coupled aeroelastic calculations using any kind of existing fluid dynamics solver, at least those providing access to their sources. The operations performed by the Aeroelastic Coupling Module (ACM) involve the consistent and conservative projection of aerodynamic loads onto the structural model, the calculation of the resulting structural deformations and the ensuing deformation of the aerodynamic surface mesh. The ACM projects the aerodynamic loads acting on the surface as well as the structural deformations by employing the point-wise principle of virtual work in combination with the shape functions used in the FE discretisation of the structure. The structural deformation is computed in form of the node-wise translations and rotations by applying an FE code. One of the numerous available free or commercial codes can easily be coupled to the ACM. Furthermore the ACM controls the coupled solution steps for different loose and tight staggered coupling algorithms and provides the ability to handle steady and time accurate unsteady aeroelastic simulations. The implementation of the ACM is available as a set of library functions directly callable from the flow solver or as an independent program version.

3   Computational Results

To prove the capabilites of SOFIA to reliably predict aeroelastic features, numerical results are compared to data gathered in the wind tunnel experiments, which were performed within the framework of SFB 401 and reported in [2]. One set of experiments is concerned with the aeroelastic equilibrium configurations of a swept elastic wing in subsonic flow. The aeroelastic equilibrium configuration is achieved when the aerodynamic loads and the structural reaction forces are in a state of equilibrium for the deformed wing model. A second set of wind tunnel tests studies the dynamic response problem of the same wing.

3.1   Wind Tunnel Model

The examined wind tunnel model was designed and having a backward sweep angle of $34°$, a
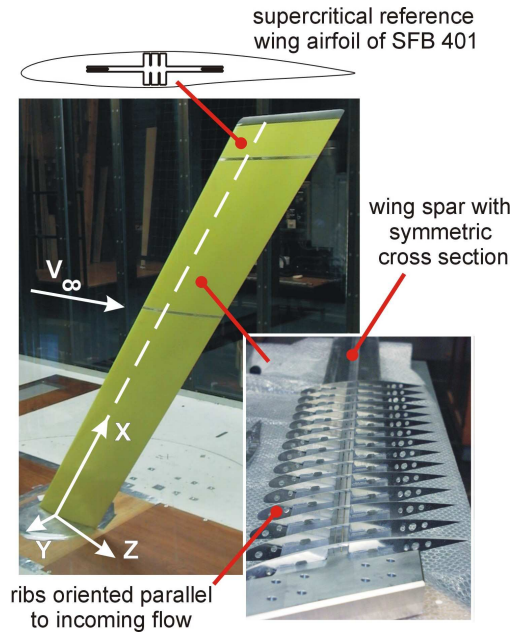
Fig. 1 Swept wind tunnel wing model mounted in German-Dutch Wind Tunnels (DNW-LST) (©ILB 2001)

half span of $1.5m$ and a chord length of $0.333m$. The chosen profile of the wing corresponds to the reference airfoil (BAC 3-11/RES/30/21) in cruise configuration chosen by the SFB 401. The structural design of the wing had to consider the demands of a desirable flexible structure with large deflections within the limits of the DNW-LST wind tunnel conditions: relatively low eigenfrequencies, very low structural damping and a wide stability range which encloses the planned test conditions. Therefore the load supporting structure is composed of a cross-shaped wing spar, as shown in Fig. 1, which is appropriate to fulfill the requirements of aeroelastic experiments of a particularly low torsional stiffness in combination with a sufficiently high bending stiffness. The transfer of aerodynamic loads to the wing spar is realized by ribs installed on the spar with positive locking and foam segments filling the space between the ribs. The orientation of the ribs is parallel to the incoming flow. The spar and the ribs are made of an aluminium alloy which garanties low structural damping and large deflections without occurence of plasticity. The structural cross-sectional properties along

the wing were determined by laboratory test series at ILB [2]. Due to the symmetric cross-section of the spar and the homogeneity of its mass distribution the centerlines of gravity, bending and torsion coincide with the centerline of symmetry. The structural dataset obtained from laboratory tests was used to identify the reduced structural Timoshenko-like beam model correspondingly to the representation of the structure within the aeroelastic method SOFIA. The ribs are imported into the simulation model by additional massless beam elements mounted at the FE representation of the spar. The projection of loads acting on the aerodynamic surface is only permitted in the simulation for the FE nodes forming a part of the ribs. Thereby the force transmission to the spar can be realised in the simulation corresponding to the experimental model. Detailed descriptions regarding the properties of the material, the cross-sectional stiffnesses along the wing length and the experimental measurement instrumentation and techniques can be found in [2].

In advance to the wind tunnel tests the identification of the model was investigated in laboratory tests under wind-off conditions. The good agreement in the deformation results after loading the spar-rib supporting configuration with a singular transverse force and a torsional moment approves the structural identification in the simulation. Secondly a modal analysis was performed in order to examine the dynamic quality of the identified beam model by means of eigenshapes and eigenvalues in comparison to the wind tunnel model. Avoiding to present the eigenshapes related to purely horizontal wing motions, Fig. 2 shows the natural vibration modes of the beam projected on the aerodynamic surface of the wing. The eigenshapes and eigenvalues of the beam model used within the aeroelastic simulation applying SOFIA are in excellent agreement with the results from experimental modal analysis for the sensor equipped wind tunnel wing model. The presented eigenfrequencies of the beam differ from the eigenfrequencies of the experimental assembly less than 0.5%.
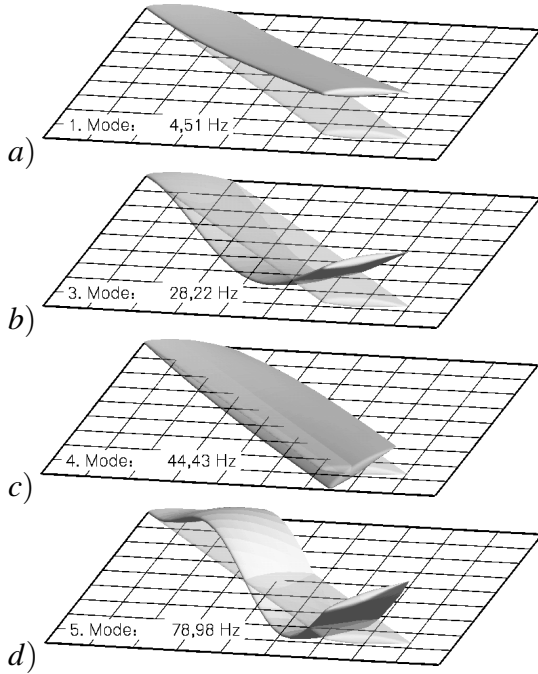
a)

b)

c)

d)

Fig. 2 Natural vibration modes of the simulated wing as a projection of the natural modes of the Timoshenko-like beam onto the wing, *a)* 1st mode, *b)* 3rd mode, *c)* 4th mode and *d)* 5th mode.

3.2 Aeroelastic Equilibrium Configurations

The following section gives a description of aeroelastic equilibrium configurations achieved by applying SOFIA to the coupled problem of the flexible swept wing in subsonic flow. The subsequent comparison is focused on results related to a flow velocitiy of $V_\infty = 75m/s$. The Reynolds number in the computations was set according to the experimental conditions to $Re_\infty = 1.75 \cdot 10^6$. Starting from the rigging root angle of incidence for vanishing lift of the aeroelastic equilibrium configuration, the rigging angle was decreased and increased in the experiments in steps of two degrees, one step below the angle with vanishing lift and five steps above. Consequently, the experimental procedure was imitated in the computations resulting in a range of rigging angles from about $\alpha_R = -3.5°$ to $+8.5°$.

Fig. 3 a) and b) show computational results for the deformation at the wing tip, i. e. the displacement u_Y^{tip} and the twist due to torsion φ_X^{tip} of

a cross-section perpendicular to the beam axis, against the angle of incidence α_R for a flow velocity of $V_\infty = 75m/s$. The symbols are related to the experimental results, whereas the lines belong to results from solving the Euler equations on the one hand and the RANS equations on the other hand. A solution to the RANS equations was produced using the one-equation turbulence model of Spalart-Allmaras. Thereby the location of transition was assumed to be at the leading edge in all considered test cases. The plotted results have in common that the solutions based on the RANS equations lead to a precise prediction of the tip displacement for all angles of incidence unlike the computations without considering the influence of boundary layers. The agreement for the twist deformation due to torsion is insignificantly incorrectly predicted. The main difference is that the slope of change of the torsional twist against the angle of incidence is not reproduced exactly. But the differences remain below $0.15°$.

In Fig. 4 a) and b) the displacements and torsional twists are plotted against the beam axis co-ordinate X for three exemplary angles of incidence. Again, the computational results from solving the Euler and RANS equations for the flow field are compared to the measured data. The comparison reveals that the good agreement regarding the prediction of deformation in case of a RANS-based simulation does not only apply for the deformation of the wing tip but also for the whole wing. However it must be noted that the torsional twist along the beam axis is approximated better by an Euler-based simulation in case of negative angles of incidence. But the difference comparing with the measured data increases when simulating the flow field using the Euler equations, at least for increased angles of incidence.

The reaction forces of the wing structure in the clamping plane were recorded by a six-components balance during the experiments. Fig. 5 a) and b) show the comparison of measured vertical force F_Y^{Root} and torsional moment M_X^{Root} to the corresponding quantities in the simulation over the whole range of angles of incidence. One can observe again that the overall agreement is
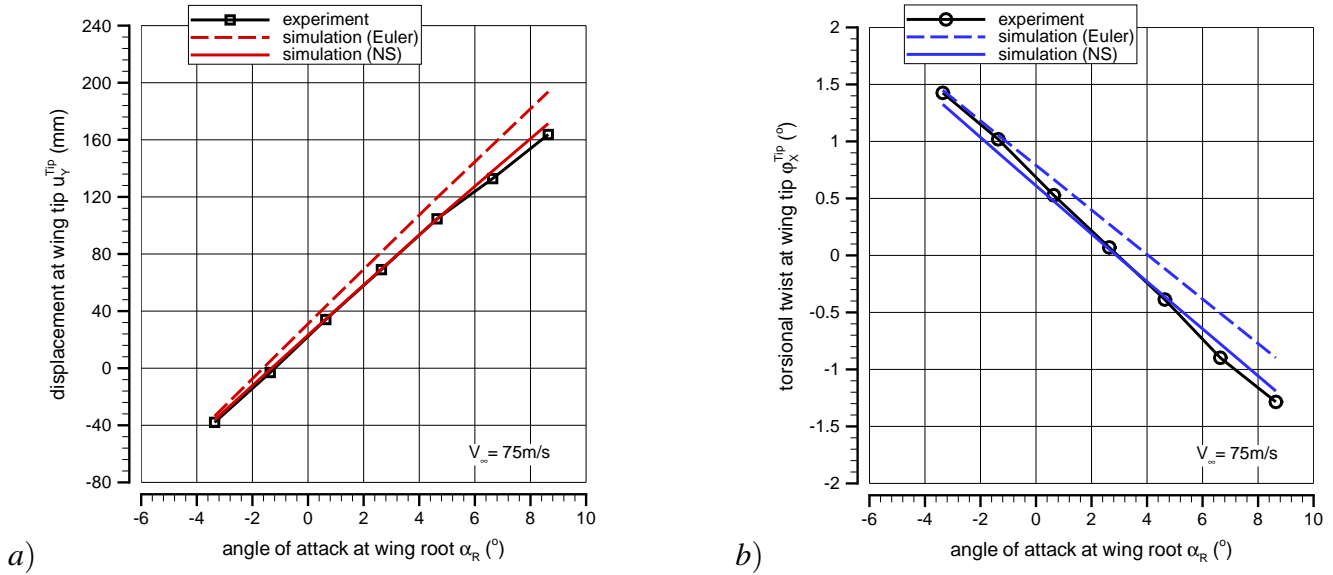
Fig. 3 Comparison of measured and computed a) displacement and b) torsional twist at the wing tip as a function of the rigging angle of incidence at wing root α_R for a flow velocity $V_\infty = 75m/s$.
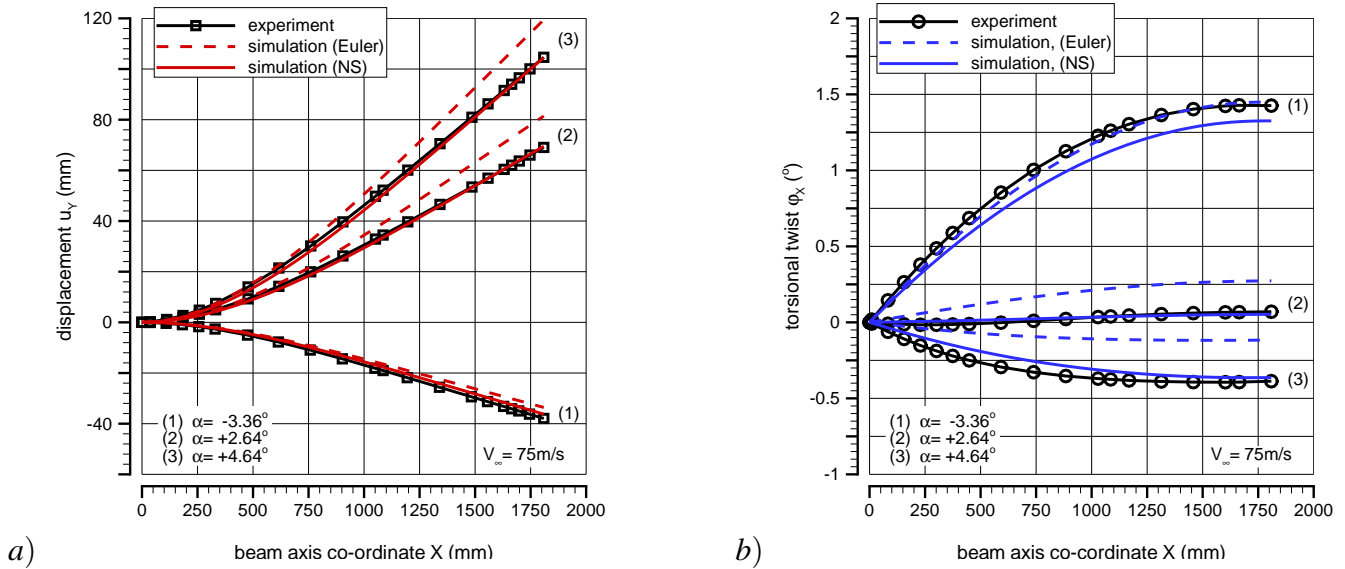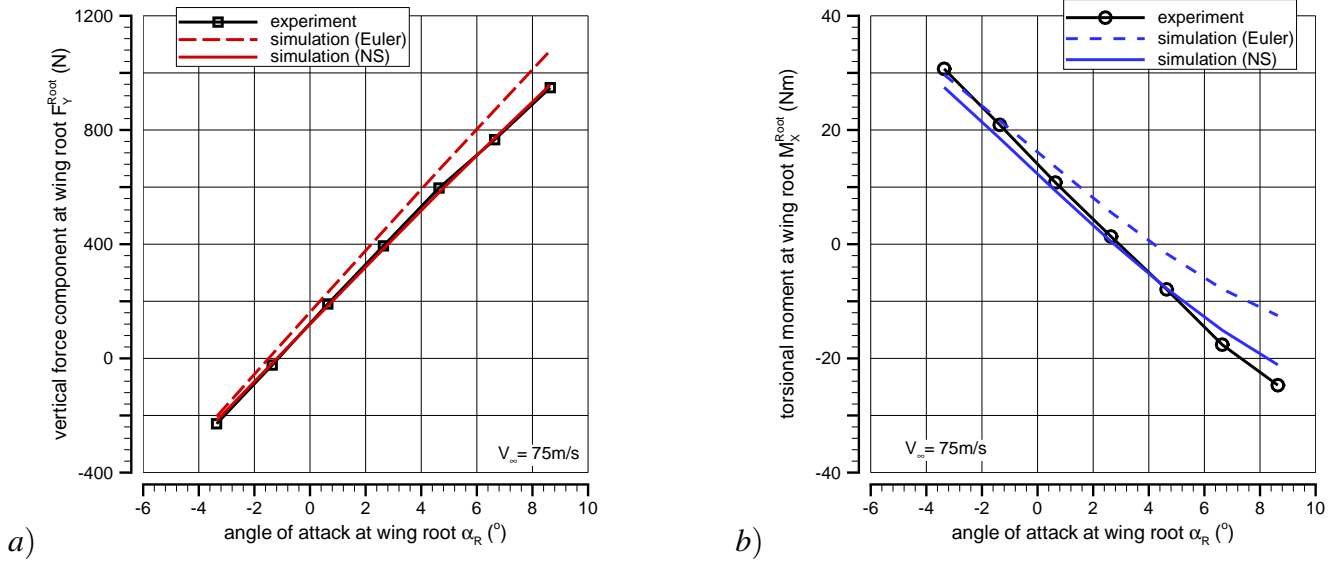
Fig. 4 Comparison of measured and computed a) vertical force component and b) torsional moment as a function of the beam axis co-ordinate for three different rigging angles of incidence and a flow velocity of $V_\infty = 75m/s$.

Fig. 5 Comparison of measured and computed a) vertical force component and b) torsional moment at the wing root as a function of the rigging angle of incidence at wing root α_R for a flow velocity of $V_\infty = 75m/s$.

good, but the differences between experimental and computional results slightly increase with an increasing angle of incidence. Anyhow those differences do not exceed $11N$ for the vertical forces and $4Nm$ for the torsional moments within the considered range of root angles of incidence.

3.3 Aeroelastic Vibrations

On part of the ILB unsteady wind tunnel tests were carried out for the swept wind tunnel model in DNW-LST implying dynamic response tests. To enforce a dynamic response of the wing at wind-on conditions, a thread has been attached to the wing tip with its action line being located outside of the elastic axis. Therefore the applied force results in an additional bending and torsional moment deforming the wing from its aeroelastic equilibrium configuration. Thus, after cutting the thread, an oscillation of the wing took place in bending and torsional twist deformation. The procedure of the experiments was imitated in the simulations by first applying a static aeroelastic computation considering the additional thread force. The resultant displacement field of the

structure and the velocity flow field constitutes the initial condition for the time-dependent simulation after removing the thread force.

Subsequently the prediction performance of the aeroelastic simulation is examined on the basis of a comparison of the computed and measured time histories of the bending deflection and the torsional twist at the wing tip, as well as the bending and torsional moment in the clamping plane. Within the sense of these announced actions Fig. 6 a) shows in solid lines the computed time history of the wing tip deflection, where b) plots the torsional twist deformation at the wing tip. The experimentally traced results are added as symbols. Likewise in the static case, the dynamic aeroelastic simulations were carried out by describing the flow field with RANS equations closed by the turbulence model of Spalart-Allmaras. The bending displacement almost coincides with the course of measured data regarding amplitude and phase. The simulation captures the kinematic coupling of bending and torsional twist oscillation very well, which can be seen from the moderately damped low-frequency contribution to the torsional twist deformation.
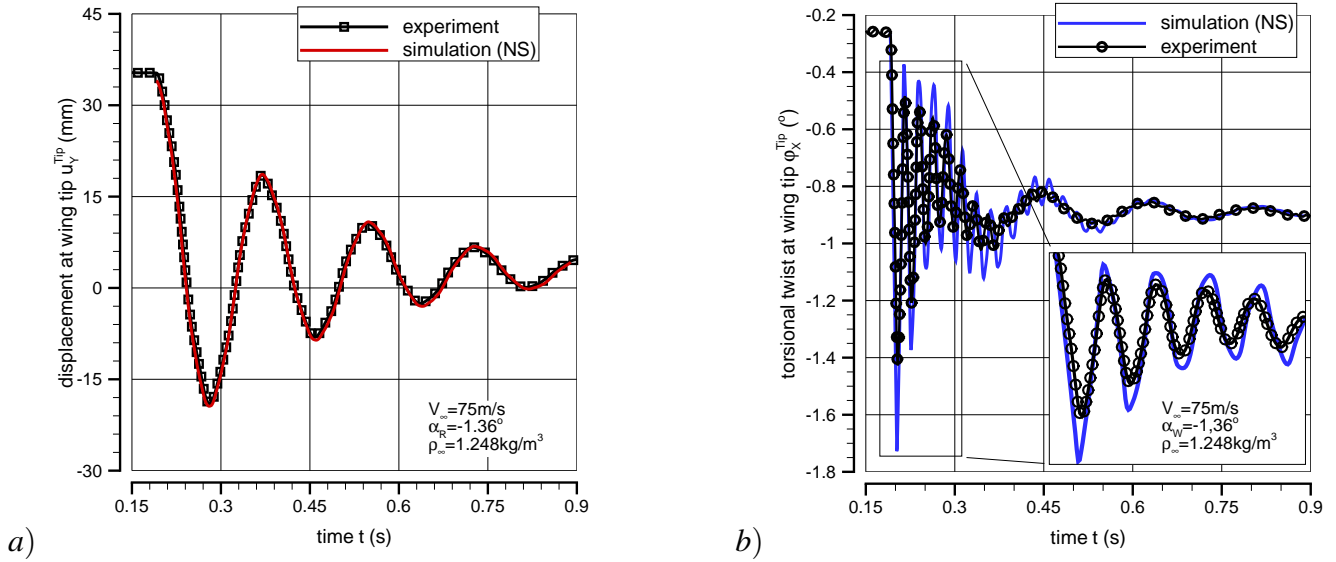
Fig. 6 Time histories of measured and computed *a)* displacements and *b)* torsional twists at wing tip for an incoming flow velocity of $V_\infty = 75m/s$.

However the enlarged detail shows the overestimation of the torsional amplitude by the simulation. The low difference in the prediction of the torsional vibration frequency results in a phase error increasing with time.

The mentioned observations are confirmed by inspecting the modal contributions to bending and torsional vibration regarding vibration frequency and aerodynamic damping. These were gained by performing a spectral analysis to the time histories of deformation for all investigated incoming flow velocities. The aerodynamic damping is defined here as the determined damping coefficient characterising the reduction of the modal amplitude within one period in percentage of the corresponding angular eigenfrequency. In continuation to the results afore Fig. 7 a) reveals an excellent agreement of computed and measured aeroelastic vibration frequencies for the first two bending modes over the whole range of studied flow velocities. However, the ascertained phase deviation of the first torsional mode grows even more with increasing flow velocity.

The corresponding time-dependent forces and moments in the clamping plane were deter-

mined in the simulation by differentiation of the spanwise bending and torsional twist deformation close to the clamping according to the constitutive equations of the internal structural forces. Fig. 8 a) and b) oppose the computational time-dependent results for the torsional moment and the bending moment respectively to the measured time histories. Consistently with the torsional twist deformation, the amplitudes of the torsional moment are less accurate, whereas the computed bending moment follows the experimentally detected behaviour very accurate.

4 Conclusions

Within the framework of the Collaborative Research Center SFB 401 the aeroelastic method SOFIA has been applied to compute the wing deformation in combination with the surrounding flow field for a swept wind tunnel wing model in subsonic flow. SOFIA uses a coupled multi-field formulation, the flow is modeled optionally by either the Euler or the Navier-Stokes equations, and the wing structure is described by a generalised quasi one-dimensional theory based on Timoshenko's beam theory. The computational
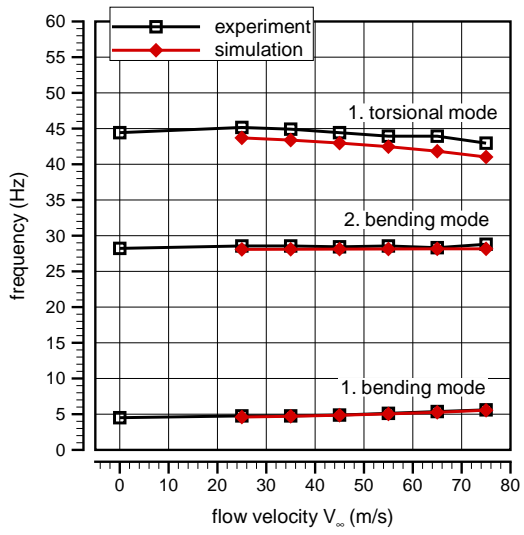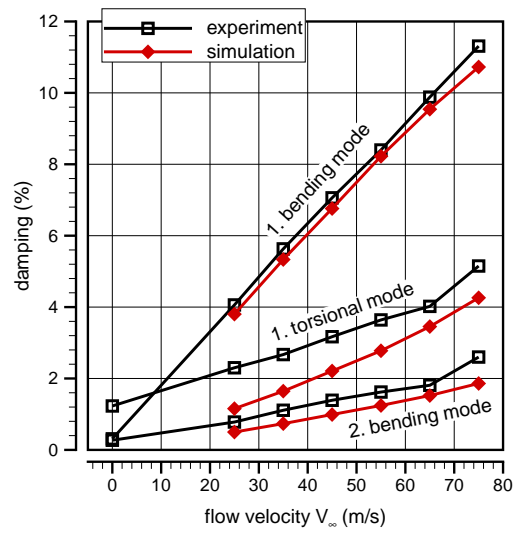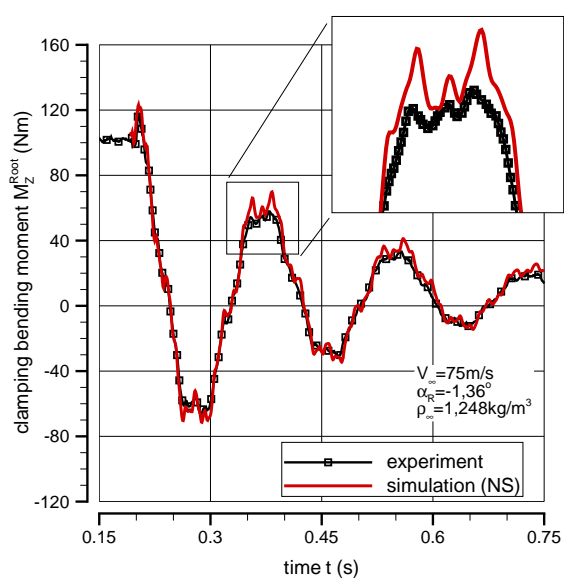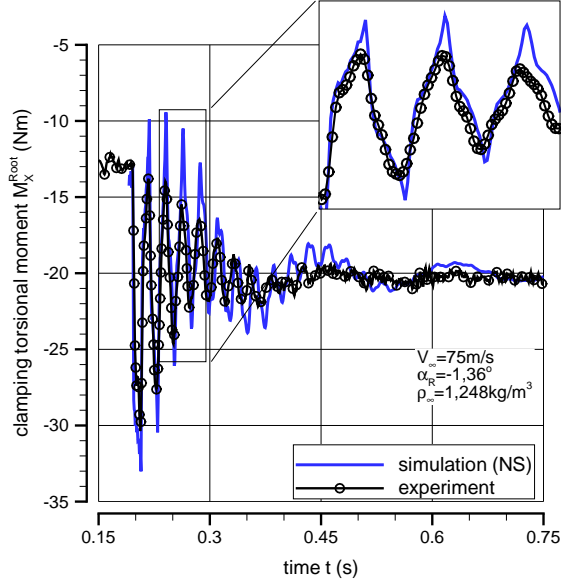
Fig. 7 Comparison of measured and computed *a*) modal frequencies and *b*) modal dampings in time histories of the wing deformation at dynamic reponse tests.

Fig. 8 Time histories of measured and computed *a*) bending and *b*) torsional moment in the clamping plane for an incoming flow velocity of $V_\infty = 75m/s$.

L. REIMER*, C. BRAUN**, J. BALLMANN**

results concerning deformations and integral re-action forces and moments obtained by applying SOFIA were compared extensively to experimental results obtained from both static and dynamic aeroelastic wind tunnel tests in DNW-LST.

The comparison of both static and dynamic computational and experimental results reflect nearly the same. All computational results originating dominantly from bending deformation are in excellent agreement with the measured data. The differences in the spanwise bending displacement of the aeroelastic equilibrium configurations do not exceed $8mm$ for deflections within a range from about $-38mm$ to $+172mm$. The deviation of the vibration frequency for the first bending mode remains below $0.07Hz$, which means less than 1.1% for all investigated incoming flow velocities. A maximum deviation of the aerodynamic damping, which is already given in percentage of the corresponding frequency, of 0.8 percentage points is reached for the first bending mode. The numerical results significantly related to the twist deformation due to torsion are predicted less precise. The main difference in the static case is that the slope of change of the torsional twist against the angle of incidence is not reproduced exactly. But the differences remain below $0.15°$ for all studied test cases, where the measured torsional deformation varies from about $-1.2°$ to $+1.4°$. In essence the deviations in the dynamic case consist of an overestimation of the amplitudes of the torsional twist and moment, accompanied by a maximum difference regarding the aerodynamic damping coefficient of 1.8 percentage points.

In addition it must be noted here that the good agreement between experiment and simulation could only be achieved on conditions, which include the viscosity of the fluid in the aeroelastic computation.

5   Acknowledgements

References

[1] Ballmann, J. (Ed.): *Flow Modulation and Fluid-Structure Interaction at Airplane Wings – Research Results of the Collaborative Research Center SFB 401 at RWTH Aachen.* Notes on Numerical Fluid Mechanics and Multidisciplanary Design (NNFM), Springer Verlag Heidelberg, Vol. 84, 2003

[2] Kämpchen, M., Dafnis, A., Reimerdes, H.-G.: *Aero-Structural Response of a Flexible Swept Wind Tunnel Wing Model in Subsonic Flow.* Proceedings of the International Forum on Aeroelasticity and Structural Dynamics (IFASD) in Amsterdam, 2003

[3] Kroll, N., Fassbender, J. K. (Eds.): *MEGAFLOW – Numerical Flow Simulation for Aircraft Design.* Notes on Numerical Fluid Mechanics and Multidisciplinary Design (NNFM), Vol. 89, Springer Verlag Heidelberg, 2005

[4] Boucke, A.: *Kopplungswerkzeuge für aeroelastische Simulationen.* Doctoral Thesis, RWTH Aachen University, 2003

[5] Hesse, M.: *Entwicklung eines automatischen Gitterdeformationsalgorithmus zur Strömungsberechnung um komplexe Konfigurationen auf Hexaeder-Netzen.* Doctoral Thesis, RWTH Aachen University, 2006

[6] Hurka, J.: *Numerische Untersuchung zur Aeroelastik dünner Platten.* Doctoral Thesis, RWTH Aachen University, 2002